Published in final edited form as:
Gait Posture. 2008 July ; 28(1): 135–143.

The effect of walking speed on muscle function and mechanical energetics

Richard R. Neptune[a,*], **Kotaro Sasaki**[a], and **Steven A. Kautz**[b,c,d]

a *Department of Mechanical Engineering, The University of Texas, 1 University Station C2200, Austin, TX, USA*

b *Department of Physical Therapy, University of Florida, Gainesville, FL, USA*

c *Brain Rehabilitation Research Center, Malcom Randall VA Medical Center, Gainesville, FL, USA*

d *Brooks Center for Rehabilitation Studies, University of Florida, Gainesville, FL, USA*

Abstract

Modulating speed over a large range is important in walking, yet understanding how the neuromotor patterns adapt to the changing energetic demands of different speeds is not well understood. The purpose of this study was to identify functional and energetic adaptations in individual muscles in response to walking at faster steady-state speeds using muscle-actuated forward dynamics simulations. The simulation data were invariant with speed as to whether muscles contributed to trunk support, forward propulsion or leg swing. Trunk support (vertical acceleration) was provided primarily by the hip and knee extensors in early stance and the plantar flexors in late stance, while trunk propulsion (horizontal acceleration) was provided primarily by the soleus and rectus femoris in late stance, and these muscle contributions all systematically increased with speed. The results also highlighted the importance of initiating and controlling leg swing as there was a dramatic increase at the higher walking speeds in iliopsoas muscle work to accelerate the leg in pre- and early swing, and an increase in the biarticular hamstring muscle work to decelerate the leg in late swing. In addition, walking near self-selected speeds (1.2 m/s) improves the utilization of elastic energy storage and recovery in the uniarticular ankle plantar flexors and reduces negative fiber work, when compared to faster or slower speeds. These results provide important insight into the neuromotor mechanisms underlying speed regulation in walking and provide the foundation on which to investigate the influence of walking speed on various neuromotor measures of interest in pathological populations.

Keywords

Gait; Muscle work; Musculoskeletal modeling; Dynamic simulation

1. Introduction

Recent modeling studies of walking at self-selected speeds have identified how individual muscles work in synergy to satisfy the task demands including body support, forward propulsion and swing initiation (e.g. [1–5]). These analyses revealed that young adults walking at a self-selected speed utilize a distribution of hip and knee extensor muscle force in early stance and ankle plantar flexor and rectus femoris force in late stance to provide support and

*Corresponding author. Tel.: +1 512 471 0848; fax: +1 512 471 8727. E-mail address: rneptune@mail.utexas.edu (R.R. Neptune).

Conflict of interest: There is no conflict of interest regarding the publication of this manuscript.

forward propulsion. However, how the muscle contributions to these important functional tasks change with walking speed is not well understood. Intuitively, walking at faster steady-state speeds would necessitate an increase in activity for muscles that contribute to forward propulsion. However, faster walking speeds are also associated with longer stride lengths (e.g. [6]), which may require increased activity from those muscles contributing to leg swing (e.g. [7]), and increased activity from those muscles contributing to vertical support because the vertical excursion of the body's center of mass increases (e.g. [8]). Conversely, walking at slower speeds may be mechanically less efficient (e.g. deviating more from natural frequency of the pendular movement so that additional muscular effort may be required) and less conducive to the storage and recovery of elastic energy in the musculotendon complex.

Analysis of muscle activity as walking speed increases has shown that the fundamental phasing relative to regions of the gait cycle remains relatively stable (e.g. [9–12]). However, walking speed influences each muscle's contractile state (i.e. fiber length and velocity), which may alter the muscle's ability to generate force and power. The potential influence of intrinsic muscle properties on muscle coordination was evident in a recent study showing that the ability of the ankle plantar flexors to produce force as walking speed increased was greatly impaired, despite an increase in muscle excitation, due to sub-optimal contractile conditions (i.e. increased muscle fiber lengths [13]). Since the plantar flexors have been shown to be important contributors to support, forward propulsion and swing initiation during normal walking [1–5], increased output from other muscle groups would appear necessary to compensate for the decreased plantar flexor output.

Understanding how the neuromotor patterns adapt to the changing energetic demands of increased walking speed is further complicated by the potential increase of elastic energy storage and recovery in tendons (e.g. [14–16]). Gait kinematics and muscle force requirements change with walking speed (e.g. [17]), which may alter the muscle tendon and fiber kinematics and vary tendon elastic energy storage and recovery. Such variations may partially offset the need for increased active force generation to walk faster. However, the muscles most sensitive to increases in walking speed have not been identified.

The goal of this study was to identify the neuromotor modifications responsible for walking at faster steady-state walking speeds using muscle-actuated forward dynamics simulations that emulate the experimentally collected data of young adults walking at a wide range of walking speeds. The dynamic simulations provide a framework to quantify individual muscle and tendon work and the biomechanical energetic mechanisms executed by each muscle to satisfy the task requirement changes with faster walking speeds. We expected the largest adaptations to occur during the stance phase, as swinging the leg during normal self-selected walking speeds is often assumed to be ballistic (e.g. [18]). However, others have suggested the metabolic cost of leg swing is significant (e.g. [19]) and could become more costly with increased walking speed as the acceleration and deceleration of the swing leg increases. Thus, identifying such functional adaptations by individual muscle groups to increasing walking speed will provide important insight into the neuromotor mechanisms underlying speed regulation in walking and provide the foundation on which to investigate the influence of speed on various neuromotor measures of interest in pathological populations.

2. Methods

2.1. Musculoskeletal model

A musculoskeletal model and dynamic optimization framework were used to generate muscle-actuated forward dynamics simulations of walking at 0.4, 0.8, 1.2, 1.6 and 2.0 m/s. The bipedal sagittal plane musculoskeletal model (Fig. 1) and optimization framework used to produce the simulations using optimal tracking have been previously described in detail [3,4]. Briefly, the

musculoskeletal model was generated using SIMM (MusculoGraphics, Inc.) [20] and consisted of rigid segments representing the trunk and legs. Each leg consisted of a thigh, shank and foot. The trunk segment included the mass and inertial characteristics of the pelvis, torso, head and arms. The musculoskeletal geometry was based on Delp et al. [21] and the system dynamical equations-of-motion were generated using SD/FAST (Symbolic Dynamics, Inc.). The contact between the foot and the ground was modeled by 30 discrete visco-elastic elements with coulomb friction attached to the bottom of each foot segment [22]. Passive torques representing the forces applied by ligaments, passive tissue and joint structures were applied at the hip, knee and ankle joints [23].

Seventeen individual Hill-type musculotendon actuators for each leg drove the model (Fig. 1), which were combined into 10 muscle groups based on anatomical classification, with muscles within each group receiving the same excitation signal. Experimentally collected EMG linear envelopes (see Section 2.3) were used to define the muscle excitation patterns. For those muscles from which EMG were not measured (IL, BFsh, GMED), a block excitation pattern was used. The muscle force generating capacity was governed by Hill-type muscle properties [24] and a first-order differential equation was used to represent the muscle activation dynamics [25].

2.2. Dynamic optimization

Dynamic optimization was used to generate the walking simulations at the five different speeds by fine-tuning the excitation onset, duration and magnitude for each muscle group using a simulated annealing algorithm [26] until the difference between the experimental and simulated kinematic and ground reaction force data was minimized (e.g. [3,4,13]). The specific quantities evaluated in the objective function included the time history of the right and left hip, knee and ankle joint angles, horizontal and vertical ground reaction forces, and the two components (x, y) of the trunk translation resulting in a total of $n = 12$ tracking variables.

2.3. Experimental data collection

The data collection procedures have been previously described [13] and will be briefly described here. Ten subjects (5 male, 5 female; age 29.6 ± 6.1 years; height 169.7 ± 10.9 cm; mass 65.6 ± 10.7 kg) walked at speeds of 0.4, 0.8, 1.2, 1.6 and 2.0 m/s on a split-belt instrumented treadmill (TecMachine, France) while muscle EMG, three-dimensional ground reaction forces (GRFs) and body segment motion data were collected using a motion capture system (Motion Analysis, Corp.) for 15 s at each randomly assigned walking speed. Prior to the data collection, all subjects provided informed consent according to the rules and regulations of the Cleveland Clinic Foundation and The University of Texas at Austin.

EMG data were collected using bipolar surface electrodes from the soleus, medial gastrocnemius, tibialis anterior, gluteus maximus, vastus medialis, biceps femoris long-head and rectus femoris. The data were band-pass filtered (20–400 Hz), fully rectified and then low-pass filtered at 10 Hz using a fourth order zero-lag digital Butterworth filter. Each EMG pattern was then normalized to its maximum value during walking at 2.0 m/s. The body segment motion data were measured using a modified Helen Hayes marker set and corresponding joint angles were determined. The GRF and motion data were filtered with a fourth order zero-lag Butterworth filter with cut-off frequencies of 20 and 6 Hz, respectively. All data were averaged across 10 consecutive walking cycles within each subject at each speed, and then across subjects to obtain a group average.

2.4. Muscle and tendon mechanical work

Positive and negative mechanical work done by the muscle fibers and tendon were obtained by time-integrating the positive and negative muscle fiber and tendon power derived from the

simulations, respectively, over the stance and swing phases of the gait cycle. Net mechanical work done by the muscle fibers was determined from the sum of the positive and negative muscle fiber work. Negative tendon work corresponded to the energy stored in the tendon while positive tendon work corresponded to the energy recovered from the tendon. The positive, negative and net fiber and positive tendon work were then summed individually across all muscles to quantify the total muscular output during stance, swing and the entire gait cycle.

2.5. Assessing muscle function

To identify the influence of walking speed on individual muscle contributions to body support, forward propulsion and leg swing, a segment power analysis was performed [27]. First, the contribution of each muscle to the ground reaction force was determined. This contribution and its corresponding center-of-pressure (needed for subsequent analyses, see below) were determined using a two-step perturbation analysis [3]. First, the total ground reaction force and center-of-pressure were calculated at time step i from the visco-elastic elements based upon the current state of the system. Then, at time step $i - 1$, all muscle forces were applied to the system except for the muscle of interest and the equations-of-motion were integrated over the time step from $i - 1$ to i ($dt = 30$ ms). The ground reaction force and center-of-pressure were subsequently recomputed for the new state of the system. The muscle's contribution to the ground reaction force and center-of-pressure were approximated by the difference in these quantities for the original and new system states. The process was then repeated for each muscle.

The segment power analysis uses a state-space approach to determine the instantaneous power of each body segment based on the time derivative of the total segmental mechanical energy, which is a function of its current state (position and velocity) and its corresponding acceleration. Therefore, the mechanical power generated, absorbed or transferred by an individual muscle to or from each segment was determined as a function of the current state of the segment and the instantaneous accelerations induced by that muscle [27]. The muscle-induced accelerations were determined by setting gravity and all velocities to zero, applying the one muscle force of interest and its corresponding contribution to the ground reaction force at its center-of-pressure, and computing the resulting segmental accelerations from the equations-of-motion using SD/FAST. Since the right and left leg muscle coordination patterns were symmetrical, the data were only analysed for the right leg muscles.

3. Results

The walking simulations at each of the five walking speeds (0.4, 0.8, 1.2, 1.6 and 2.0 m/s) emulated well the group-averaged kinematics and ground reaction forces (e.g. Fig. 1) similar to our previously published work (e.g. [3,4,13,28]). The corresponding muscle excitation patterns also closely mimicked the EMG linear envelopes, which generally increased in magnitude as walking speed increased (Fig. 2). The exceptions were BFsh and GMED, and RF and VAS in late swing, which did not change significantly with speed.

3.1. Musculotendon work

During the stance phase, the total positive, negative and net fiber work and recovered tendon elastic energy systematically increased with speed beyond 0.8 m/s (Fig. 3). During the swing phase, total positive and negative fiber work also increased with speed, although the net work remained relatively constant. Note, the net fiber work equals the net musculotendon work (MTnet) over the gait cycle since the net tendon work is zero (i.e. it is passive). The amount of positive fiber work in stance was much greater than during swing. However, as walking speed increased, the percent difference decreased. For example, at the slowest walking speed

of 0.4 m/s, the amount of concentric fiber work during stance was nearly 200% greater than during swing. However, at the fastest walking speed of 2.0 m/s, the difference was only 150%.

The plantar flexors (SOL and GAS) and hip extensors (HAM and GMAX) were the primary contributors to positive fiber work during stance, while RF and VAS were the primary contributors to negative work (Fig. 4A). During swing, the primary contributor to positive fiber work was IL, while HAM was the primary contributor to negative work (Fig. 4B). Some muscle groups were more sensitive than others to changes in walking speed, with those muscles that showed the largest speed-related changes in muscle work also showing the largest speed-related changes in muscle excitation. The fiber work from SOL (positive) and GMAX (positive) in stance and TA (positive), IL (positive) and HAM (negative) in swing changed the most with increasing speed (Fig. 4). Across all muscles, SOL stored and recovered the largest amount of elastic energy, with the largest amount occurring at 1.2 m/s. GAS and HAM elastic energy storage was similar at the higher speeds while VAS and GMAX storage increased with speed, although the energy stored in these muscles was much less. There was very little elastic energy stored and recovered in any muscle during swing (Fig. 3).

3.2. Muscle function

Although there were some quantitative differences, all muscles generated consistent body segment mechanical energetics and contributions to body support and forward propulsion as walking speed increased, which was consistent with our previous studies of muscle function [3–5]. The hip and knee extensors (VAS and GMAX) and the plantar flexors (SOL and GAS) were the primary contributors to trunk support in early and late stance, respectively. Of particular interest was each muscle's contribution to trunk forward propulsion with increased walking speed, which was provided primarily by SOL and RF in late stance (Fig. 5). SOL and RF contributions to trunk propulsion systematically increased with walking speed. Leg swing initiation was provided by GAS and IL, as they both acted to deliver energy to the leg in pre-swing (Fig. 6). IL had the largest increase in its contribution to the body segment mechanical energetics with walking speed of all muscles while HAM acted strongly at the faster speeds to decelerate the leg in late swing in preparation for heel-strike (Fig. 6).

4. Discussion

Analysis of individual muscle energetics showed SOL had the largest positive fiber work output among all muscles during stance and it systematically increased with speed (Fig. 4A), which is consistent with its role to provide trunk forward propulsion [3,5]. GAS and RF work output also increased with speed, which is to be expected because of their synergism to provide trunk forward propulsion [4,5]. SOL and GAS activity was relatively stable during mid-stance with increasing walking speeds, as SOL and GAS primarily contribute to support then (e.g. [3]). However, in late stance, their activity increased significantly with speed, which is consistent with their function to provide the majority of forward propulsion and swing initiation [2,3,5].

Elastic energy storage and recovery in the plantar flexors appears to be an effective mechanism to reduce a portion of the positive muscle fiber work necessary to provide body support and forward propulsion in late stance. For example, when increasing speed from 0.8 to 1.2 m/s, tendon accounted for ~7 J of increased positive work while the muscle fiber work increased by ~6 J (Fig. 3). SOL had the largest elastic energy storage and recovery among all muscles during stance, which had a general trend to increase with walking speed (Fig. 4A). An interesting note is that SOL stored the most elastic energy in its tendon at 1.2 m/s, which is near the optimal speed for minimizing energy expenditure during walking per unit distance (e.g. [29]). The differences in elastic energy storage and recovery between SOL and GAS are consistent with previous results in the literature. Ishikawa et al. [16] showed that the tendinous tissues of both GAS and SOL lengthened throughout single-stance phase and then recoiled

rapidly during pre-swing. However, the fascicle length changes demonstrated different patterns and amplitudes between the two muscles. The medial gastrocnemius fascicles were stretched during the early single-stance phase and then remained isometric in late stance. In contrast, the soleus fascicles were lengthened until the end of the single-stance phase. As a result, the SOL tendon strain was greater than GAS.

A surprising finding was the lack of elastic energy storage and recovery by the hip flexors in pre- and early swing. Examination of the musculotendon dynamics showed IL was not stretched enough during stance to store significant elastic energy. However, the passive hip joint torque in our model, which represents the forces applied by ligaments, passive tissue and joint structures, did store elastic energy that increased with walking speed. The energy recovery coincided with IL muscle power in pre- and early swing that reduced the necessary muscle fiber work from IL to accelerate the leg into swing. A sensitivity analysis was performed on the stiffness of the passive hip joint torque, which showed that as stiffness decreased, the required IL work increased. Thus, the amount of required IL work to facilitate leg swing is dependent on the passive hip joint and tendon stiffness and may vary across subjects.

Another interesting observation was that total negative muscle work was minimized during stance near 1.2 m/s (Fig. 3) and increased beyond that speed. This was the result of increased negative muscle work that occurred during the loading response as stride length increased, and was perhaps because of activation–deactivation dynamics that limits the rate at which muscle force can deactivate [30]. Similarly, walking at speeds below 1.2 m/s increased negative fiber work. Thus, the overall system may be inherently more stable at self-selected speeds near 1.2 m/s and require less co-contraction from the muscles to stabilize the system. In addition, increasing walking speed from the slow speeds characteristic of some impaired populations may have implications for improved efficiency.

We expected the largest adaptations in muscle work would occur during the stance phase, as swinging the leg is often assumed to be largely ballistic and the net power output of swing-phase muscles during normal walking speeds is relatively low compared to stance (e.g. [4]). The simulation data showed that indeed, the largest amount of fiber work occurred in stance (Fig. 3). However, there was considerable positive and negative work during swing, especially at the higher speeds, and the percent difference in concentric fiber work between stance and swing decreased as walking speed increased (Fig. 3).

The increase in positive fiber work in swing was due to primarily IL accelerating the leg forward in early swing while the increase in negative work was due to primarily HAM decelerating the leg in late swing in preparation for the loading response (Fig. 6). Note that the initial deceleration caused by HAM at the higher walking speeds is due to passive force generation as the hip becomes more flexed at the end of the swing phase. This increased hip flexion combined with knee extension stretches the muscle beyond its rest length, which creates a passive force that decelerates the leg. The results for IL and HAM were consistent with previous data showing increased positive hip and negative knee joint power in early and late swing, respectively, with increased walking speed [31]. The increase in fiber work would be expected, considering that step length increases dramatically as walking speed increases [6,32] (Fig. 1). The simulation step length, which corresponds with the human subject data, increased from 0.38 m at 0.4 m/s to 0.89 m at 2.0 m/s. This increase in step length required more power from those muscles contributing to leg swing, which was observed in GAS in pre-swing and IL in pre- and early swing (Fig. 6). Doke et al. [7] estimated that moving the legs represents nearly 1/3 of the total energetic cost of walking at 1.3 m/s, while Umberger [33] used a model of metabolic cost and estimated that 29% of the total metabolic cost of walking occurs during swing. These results are consistent with our simulation results, which showed muscle work

generated during swing ranged from 25% to 29% of the total positive concentric work done over the gait cycle.

The hip flexors appear to be an important compensatory mechanism for decreased plantar flexor output at higher walking speeds. GAS, which is an important contributor to swing initiation [3,4], did not have as large of an increase in muscle work as IL, despite a similar increase in excitation (Fig. 2). Previous simulation work has shown this is due to its poor contractile state as walking speed increases [13]. Thus, the functional role of IL to accelerate the leg into swing becomes more important as the contribution of GAS decreases at higher walking speeds. This is consistent with pathological populations where impaired plantar flexor output is a limiting factor in obtaining higher walking speeds and the hip flexors provide an important compensatory mechanism (e.g. [34]). Similarly, recent simulation analyses of below-knee amputee gait have shown the hip flexors (RF and IL) to be essential in restoring a normal gait pattern in the absence of the plantar flexors (SOL and GAS) [35].

The analysis also showed that although there were some quantitative differences, all muscles generated consistent body segment mechanical energetics and contributions to body support and forward propulsion as walking speed increased. However, a potential limitation of this study is that we used a sagittal plane model to simulate walking. This was deemed appropriate since the majority of muscle work during walking occurs in the sagittal plane [36] and the functions of interest were limited to the sagittal plane (i.e. body support, forward propulsion and leg swing). However, the transverse and coronal plane motions of healthy subjects typically vary with walking speed. Thus, it is possible that the muscles we studied may have different functional roles with regard to out of plane movement or that their functional roles might have been defined differently had out of plane movement been allowed. Therefore, assessing the influence of transverse and coronal plane motions on muscle function is an important area of future work.

The results of this study highlight the importance of initiating and controlling leg swing by the dramatic increase in IL, and to a lesser extent GAS, muscle work to accelerate the leg in pre- and early swing, and HAM to decelerate the leg in late swing in preparation for heel-strike. The simulations also showed the functional roles of individual muscles remain invariant with walking speed. Body support is provided primarily by the hip and knee extensors in early stance and the plantar flexors in late stance, while trunk propulsion is provided primarily by SOL and RF in late stance, which systematically increases with speed. In addition to these changes with increasing walking speed, walking near normal self-selected walking speeds (1.2 m/s) improves the utilization of elastic energy storage and recovery in the uniarticular ankle plantar flexors and reduces negative fiber work, when compared to faster or slower speeds. These results provide important insight into the neuromotor mechanisms underlying speed regulation in walking and provide the foundation on which to investigate the influence of walking speed on various neuromotor measures of interest in pathological populations.

Acknowledgements

This work was supported by The Whitaker Foundation and NIH grant R01 HD46820. The authors also gratefully acknowledge Felix Zajac for his helpful comments on the manuscript.

References

1. Anderson FC, Pandy MG. Individual muscle contributions to support in normal walking. Gait Posture 2003;17:159–69. [PubMed: 12633777]
2. Liu MQ, Anderson FC, Pandy MG, Delp SL. Muscles that support the body also modulate forward progression during walking. J Biomech 2006;39:2623–30. [PubMed: 16216251]

3. Neptune RR, Kautz SA, Zajac FE. Contributions of the individual ankle plantar flexors to support, forward progression and swing initiation during walking. J Biomech 2001;34:1387–98. [PubMed: 11672713]
4. Neptune RR, Zajac FE, Kautz SA. Muscle force redistributes segmental power for body progression during walking. Gait Posture 2004;19:194–205. [PubMed: 15013508]
5. Zajac FE, Neptune RR, Kautz SA. Biomechanics and muscle coordination of human walking. Part II Lessons from dynamical simulations and clinical implications. Gait Posture 2003;17:1–17. [PubMed: 12535721]
6. Murray MP, Mollinger LA, Gardner GM, Sepic SB. Kinematic and emg patterns during slow, free, and fast walking. J Orthop Res 1984;2:272–80. [PubMed: 6491818]
7. Doke J, Donelan JM, Kuo AD. Mechanics and energetics of swinging the human leg. J Exp Biol 2005;208:439–45. [PubMed: 15671332]
8. Orendurff MS, Segal AD, Klute GK, Berge JS, Rohr ES, Kadel NJ. The effect of walking speed on center of mass displacement. J Rehabil Res Dev 2004;41:829–34. [PubMed: 15685471]
9. den Otter AR, Geurts AC, Mulder T, Duysens J. Speed related changes in muscle activity from normal to very slow walking speeds. Gait Posture 2004;19:270–8. [PubMed: 15125916]
10. Hof AL, Elzinga H, Grimmius W, Halbertsma JP. Speed dependence of averaged emg profiles in walking. Gait Posture 2002;16:78–86. [PubMed: 12127190]
11. Nilsson J, Thorstensson A, Halbertsma J. Changes in leg movements and muscle activity with speed of locomotion and mode of progression in humans. Acta Physiol Scand 1985;123:457–75. [PubMed: 3993402]
12. Yang JF, Winter DA. Surface emg profiles during different walking cadences in humans. Electroencephalogr Clin Neurophysiol 1985;60:485–91. [PubMed: 2408847]
13. Neptune RR, Sasaki K. Ankle plantar flexor force production is an important determinant of the preferred walk-to-run transition speed. J Exp Biol 2005;208:799–808. [PubMed: 15755878]
14. Fukunaga T, Kubo K, Kawakami Y, Fukashiro S, Kanehisa H, Maganaris CN. In vivo behaviour of human muscle tendon during walking. Proc Biol Sci 2001;268:229–33. [PubMed: 11217891]
15. Hof AL, Van Zandwijk JP, Bobbert MF. Mechanics of human triceps surae muscle in walking, running and jumping. Acta Physiol Scand 2002;174:17–30. [PubMed: 11851593]
16. Ishikawa M, Komi PV, Grey MJ, Lepola V, Bruggemann GP. Muscle-tendon interaction and elastic energy usage in human walking. J Appl Physiol 2005;99:603–8. [PubMed: 15845776]
17. Lelas JL, Merriman GJ, Riley PO, Kerrigan DC. Predicting peak kinematic and kinetic parameters from gait speed. Gait Posture 2003;17:106–12. [PubMed: 12633769]
18. Mochon S, McMahon TA. Ballistic walking: an improved model. Math Biosci 1980;52:241–60.
19. Marsh RL, Ellerby DJ, Carr JA, Henry HT, Buchanan CI. Partitioning the energetics of walking and running: swinging the limbs is expensive. Science 2004;303:80–3. [PubMed: 14704426]
20. Delp SL, Loan JP. A graphics-based software system to develop and analyze models of musculoskeletal structures. Comput Biol Med 1995;25:21–34. [PubMed: 7600758]
21. Delp SL, Loan JP, Hoy MG, Zajac FE, Topp EL, Rosen JM. An interactive graphics-based model of the lower extremity to study orthopaedic surgical procedures. IEEE Trans Biomed Eng 1990;37:757–67. [PubMed: 2210784]
22. Neptune RR, Wright IC, van den Bogert AJ. A method for numerical simulation of single limb ground contact events: application to heel-toe running. Comput Method Biomech Biomed Eng 2000;3:321–34.
23. Davy DT, Audu ML. A dynamic optimization technique for predicting muscle forces in the swing phase of gait. J Biomech 1987;20:187–201. [PubMed: 3571299]
24. Zajac FE. Muscle and tendon: properties, models, scaling, and application to biomechanics and motor control. Crit Rev Biomed Eng 1989;17:359–411. [PubMed: 2676342]
25. Raasch CC, Zajac FE, Ma B, Levine WS. Muscle coordination of maximum-speed pedaling. J Biomech 1997;30:595–602. [PubMed: 9165393]
26. Goffe WL, Ferrier GD, Rogers J. Global optimization of statistical functions with simulated annealing. J Econometrics 1994;60:65–99.

27. Fregly BJ, Zajac FE. A state-space analysis of mechanical energy generation, absorption, and transfer during pedaling. J Biomech 1996;29:81–90. [PubMed: 8839020]

28. Sasaki K, Neptune RR. Differences in muscle function during walking and running at the same speed. J Biomech 2006;39:2005–13. [PubMed: 16129444]

29. Ralston HJ. Energy-speed relation and optimal speed during level walking. Int Z Angew Physiol 1958;17:277–83. [PubMed: 13610523]

30. Neptune RR, Kautz SA. Muscle activation and deactivation dynamics: The governing properties in fast cyclical human movement performance? Exerc Sport Sci Rev 2001;29:76–80. [PubMed: 11337827]

31. Winter, DA. The biomechanics and motor control of human gait: normal, elderly and pathological. Waterloo, Ontario: Waterloo Biomechanics; 1991.

32. van Hedel HJ, Tomatis L, Muller R. Modulation of leg muscle activity and gait kinematics by walking speed and bodyweight unloading. Gait Posture 2006;24:35–45. [PubMed: 16099161]

33. Umberger, BR. The cost of swinging the leg in human walking. American society of biomechanics annual conference proceedings CD; 2006.

34. Nadeau S, Gravel D, Arsenault AB, Bourbonnais D. Plantarflexor weakness as a limiting factor of gait speed in stroke subjects and the compensating role of hip flexors. Clin Biomech 1999;14:125–35.

35. Zmitrewicz RJ, Neptune RR, Sasaki K. Mechanical energetic contributions from individual muscles and elastic prosthetic feet during symmetric unilateral transtibial amputee walking: a theoretical study. J Biomech 2006;40:1824–31. [PubMed: 17045595]

36. Eng JJ, Winter DA. Kinetic analysis of the lower limbs during walking: what information can be gained from a three-dimensional model? J Biomech 1995;28:753–8. [PubMed: 7601875]

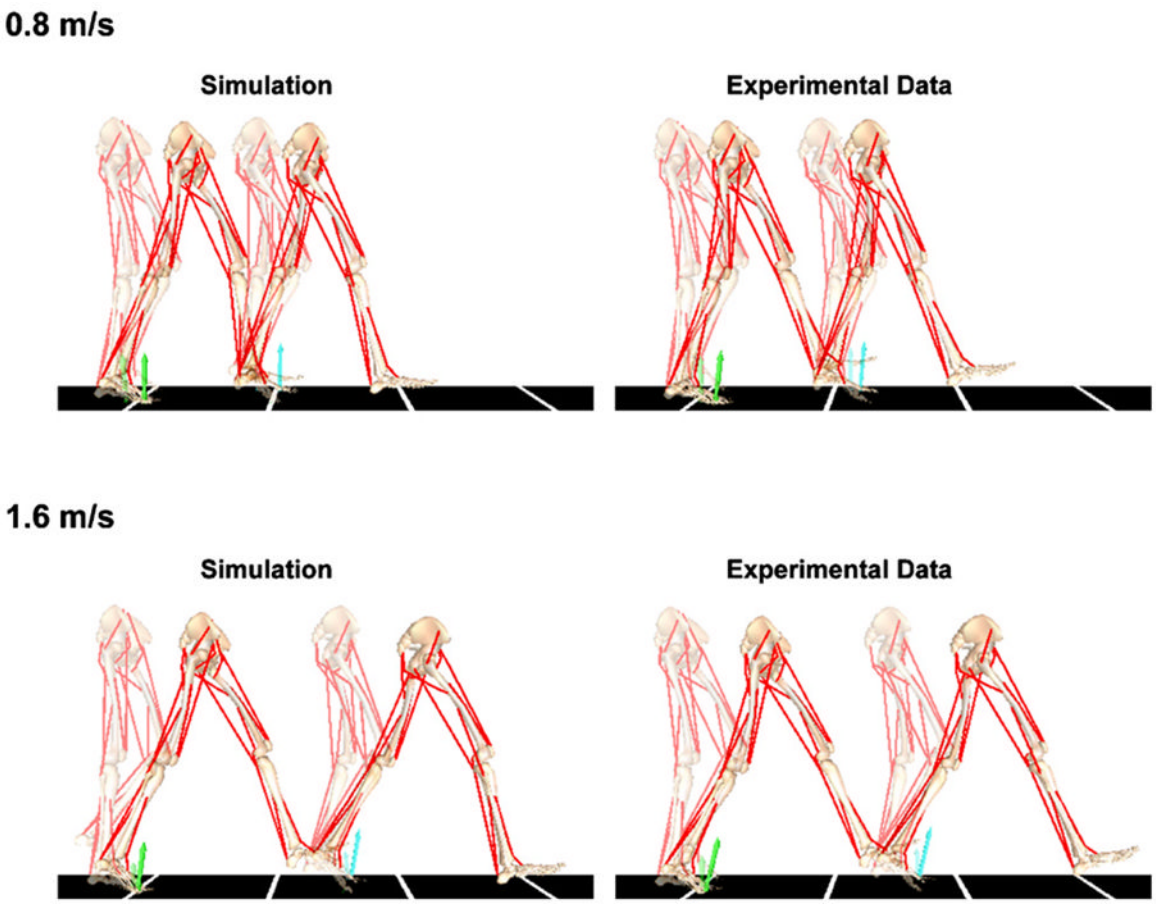

Fig. 1.

Muscle-driven simulations of walking and corresponding experimental data from right mid-stance to right heel-strike at 0.8 and 1.6 m/s. The musculoskeletal model was driven by 17 Hill-type musculotendon actuators per leg that were combined into the 10 muscle groups shown. The 10 muscle groups were defined as IL (iliacus, psoas), GMAX (gluteus maximus, adductor magnus), GMED (anterior and posterior components of gluteus medius), VAS (3-component vastus), HAM (medial hamstrings, biceps femoris long-head), SOL (soleus), BFsh (biceps femoris short head), GAS (medial and lateral gastrocnemius), RF (rectus femoris) and TA (tibialis anterior). The experimental ground reaction force vectors are shown using the simulation center-of-pressure since the experimental center-of-pressure data was not available from the treadmill measurements.

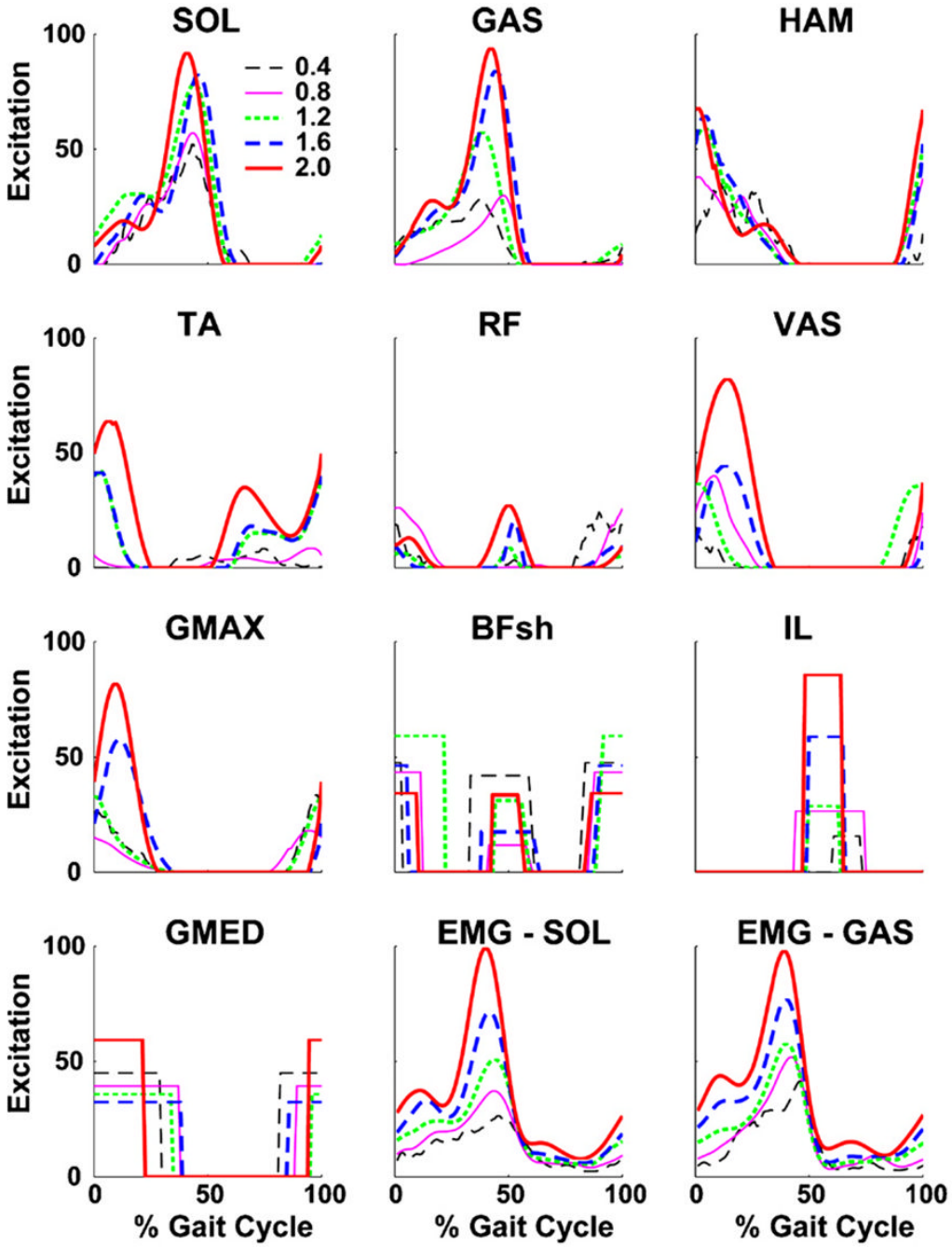

Fig. 2.

Simulation muscle excitation patterns across walking speeds. Also shown are the corresponding EMG patterns for the soleus (EMG-SOL) and gastrocnemius (EMG-GAS) to show how the simulation excitation patterns and changes with walking speed are similar to the experimentally collected EMG data.

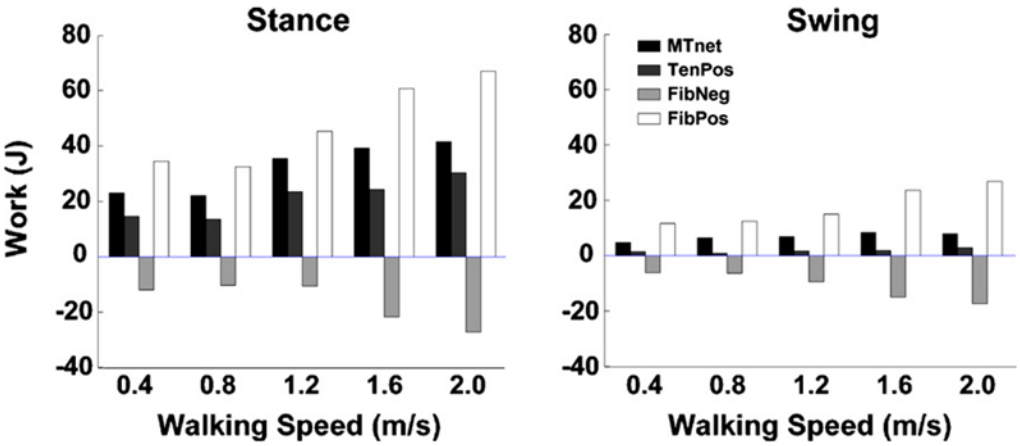

Fig. 3.

Total muscle fiber and tendon work across walking speeds (net musculotendon work (MTnet), positive tendon work (TenPos, elastic energy recovered from the tendon), negative fiber work (FibNeg) and positive fiber work (FibPos)).

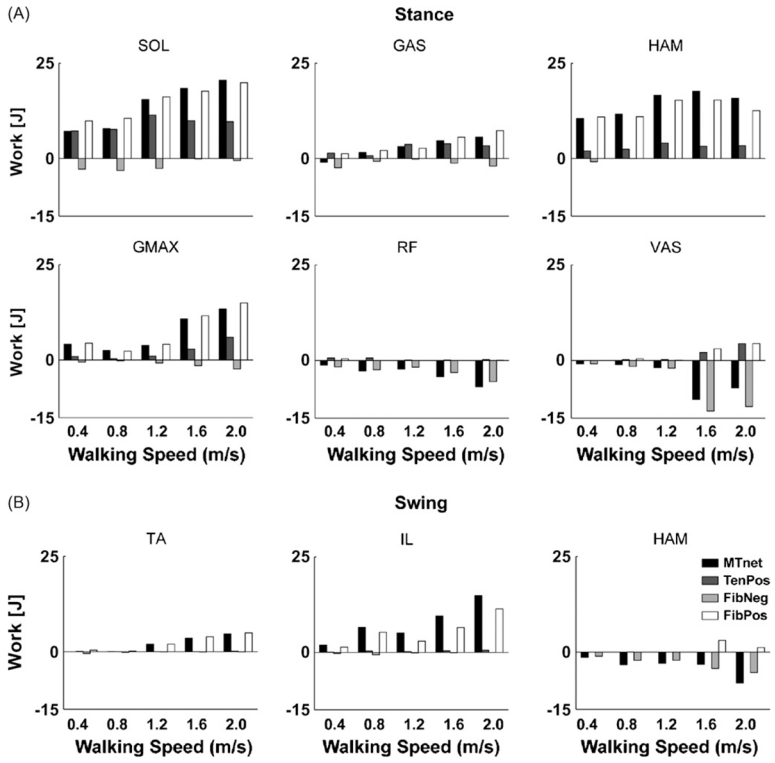

Fig. 4.

Individual muscle fiber and tendon work across walking speeds during (A) stance and (B) swing (net musculotendon work (MTnet), positive tendon work (TenPos, elastic energy recovered from the tendon), negative fiber work (FibNeg) and positive fiber work (FibPos)).

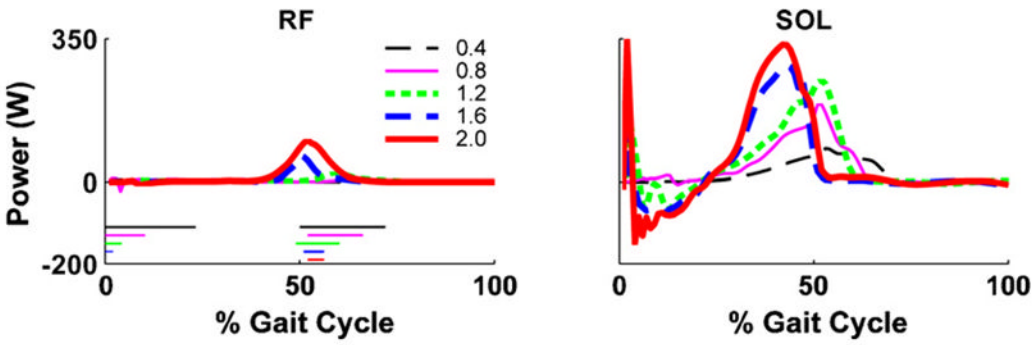

Fig. 5.

Mechanical power delivered to the trunk in the horizontal direction to provide forward propulsion by SOL and RF across increasing walking speeds. The horizontal bars indicate the regions of double support, which decreased in duration with increasing speed.

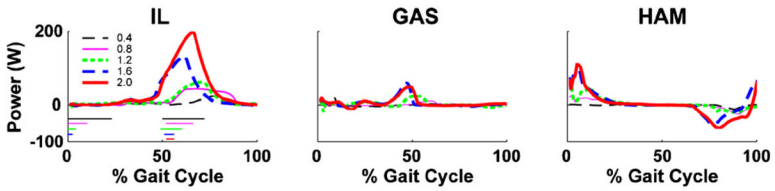

Fig. 6.

Mechanical power delivered to the ipsilateral leg by IL, GAS and HAM across walking speeds. The horizontal bars indicate the regions of double support, which decreased in duration with increasing speed. Positive (negative) power indicates the muscle acted to accelerate (decelerate) the leg in the direction of its motion.